First quantitative assessment of growth, sugar accumulation and malate breakdown in a single ripening berry

Rezk Shahood, Laurent Torregrosa, Stefania Savoi, Charles Romieu

Received: 18 June 2020 | Accepted: 9 September 2020 | Published: 20 November 2020
DOI:10.20870/oeno-one.2020.54.4.3787

OENO One
VINE AND WINE OPEN ACCESS JOURNAL

First quantitative assessment of growth, sugar accumulation and malate breakdown in a single ripening berry

Rezk Shahood [1,2], Laurent Torregrosa[1,3], Stefania Savoi[1], Charles Romieu[1,3]*

[1] AGAP, University of Montpellier, CIRAD, INRAe, Institut Agro, Montpellier, France
[2] General Commission for Scientific Agricultural Research, Lattakia, Syria
[3] GENOVIGNE, University of Montpelier, IFV, INRAe, Institut Agro, Montpellier, France

*corresponding author: charles.romieu@inrae.fr

ABSTRACT

Background: Most approaches to grape physiology accept that the berry and the future harvest should display identical developmental features, which obviously requires synchronised fruits.
Aims: Rejecting this assumption compels to revisit the kinetic and metabolic bases of berry ripening.
Methods and Results: Two to three thousand berries were individually analysed for sugar, malate and weight. The huge heterogeneity in sugar and malic acid concentrations among fruits was mostly explained by time lags in the onset of sugar storage, which proved nearly as long as the second growth phase. Individual berries from different cultivars displayed similar kinetics following the normalisation of their maximal volume. Phloem sucrose unloading started at its maximum speed at softening, but growth resumed one week later. Four hexoses accumulated per malic acid, which was oxidised during the first two weeks of ripening, and then malate breakdown stopped without affecting sugar accumulation. Sugar and water accumulation were simultaneously arrested four weeks after softening, at 0.9 M hexose, at which point sugar concentration continued through water losses.
Conclusions: The accepted sequential random sampling methods representative of average fruit and future wine compositions have led to a scrambled vision of grape developmental biology, presenting serious kinetic and composition biases. Single berry composition provides first quantitative evidence for the induction of a dominant H^+/sucrose exchange on the tonoplast, which is first electro-neutralised by malate breakdown, then by ATP demanding H^+ recirculation, in line with functional and molecular studies.
Significance of the Study: The kinetics of single berry ripening are presented for the first time. A more reliable and reproducible model of berry growth, sugar import and malate breakdown is shown here, which have definitively been improved from a quantitative point of view. It illustrates that the temporal structure of a berry population may largely contribute to future wine quality, in addition to metabolic plasticity, thereby providing another target for the impact of GxE interaction. In this respect, addressing the structure of berry cohorts may provide a new approach regarding the developmental biology/terroir nexus.

KEYWORDS

primary metabolism, growth, sugar, malate, metabolic flux, phloem unloading

Supplementary data can be downloaded through: https://oeno-one.eu/article/view/3787

INTRODUCTION

Grapevine is a non-climacteric fruit, since it neither exhibits a respiratory climax, nor an autocatalytic emission of ethylene while ripening. Due to its negligible starch reserves, grape ripens at the expense of a sudden activation of sugar unloading through the phloem apoplastic pathway (Ollat & Gaudillere, 1998; Keller & Shrestha, 2014; Zhang *et al.*, 2006). Consequently, its osmotic pressure decreases from -0.9 to -3 MPa, which enables the ripening berry to grow even under severe water deprivation (Matthews *et al.*, 1987; Keller *et al.*, 2015). Sugar accumulation immediately follows berry softening and relaxation of turgor pressure (Coombe, 1987; Gambetta *et al.*, 2010). This sequence is blocked when berries are jacketed in plastic boxes (Thomas *et al.*, 2008; Matthews *et al.*, 2009), which suggests that growth resumption is needed for the activation of phloem mass flow. This would not be the case during the ripe stage since sugar accumulation would continue after growth cessation during late ripening, thus the excess water must be rejected by xylem back-flow (Keller *et al.*, 2015; McCarthy & Coombe, 1999).

The breakdown of malic acid, which has accumulated during the green stage, usually begins almost simultaneously with sugar accumulation, but it is delayed by unusually cold temperatures, which improve the plant carbohydrate status by inhibiting respiration more than photosynthesis (Rienth *et al.*, 2016; Luchaire *et al.*, 2017). Moreover, as malate breakdown does not occur in *Vitis riparia* or *Vitis cinerea* berries, which remain highly acidic during ripening (Burzynski-Chang *et al.*, 2020), nor in the acidless *Vitis vinifera* cv. Gora chirine (Diakou *et al.*, 1997), it is not strictly required for sugar accumulation, depending on the genotype and source-sink interactions. The decrease in malic acid would result from a shift in membrane transport and energetics in *Vitis vinifera*. Even though vacuoles appear to be exceptionally impermeable to protons during the green stage, as they keep their internal acidity when undergoing an energy shortage, H^+ conductance develops during ripening. This forces the vacuolar pH to alkalinise, despite V-ATPase and H^+-PPiase gene expression, peptides and vectorial activities noticeably increase (Terrier *et al.*, 2005; Kuang *et al.*, 2019). Malic acid released into the cytoplasm then serves as a substrate for respiration or gluconeogenesis (Famiani *et al.*, 2014), and the possible excess cytoplasmic acidity can be detoxified via the formation of a diffusible pool of ethanol (Terrier *et al.*, 2005). Moreover, enzymes in the sugar/malate interconversion pathway, such as PEPcase (Phosphoenolpyruvate carboxylase), PPCKase (Phosphoenolpyruvate carboxylase kinase), ME (Malic enzyme) and MDH (Malate dehydrogenase), members of the ALMT and P3A-ATPase families, display concerted changes in gene expression, together with ADHs (Alcohol dehydrogenases) (Tesnière & Verriès, 2000; Sweetman *et al.*, 2009; Rienth *et al.*, 2016). The elucidation of the sugar/malate relationship in grapevine is complicated by the fact that both electrogenic (proton-coupled; *i.e.*, energy consuming) and non-electrogenic sugar transporters form a very versatile system, the activities and tissue organisation of which remain unknown (Afoufa-Bastien *et al.*, 2010; Lecourieux *et al.*, 2010; Kuang *et al.*, 2019). While such uncertainty makes it difficult to infer the energy cost of sugar loading in berries, it was recently hypothetised that the "phloem K^+ battery" may compensate for the supposed inability of the malic acid oxidative pathway to provide such energy (Nieves-Cordones *et al.*, 2019).

Deciphering the respective timings and intensities of major metabolic flows is, in this respect, critical to understanding the physiology of acidic fruits and targeting realistic breeding goals. It is widely accepted that berries require a ripening period of 45 ± 5 days in order to reach 1.1 M hexose concentration (Davies & Robinson, 1996; McCarthy & Coombe, 1999; Coombe & McCarthy, 2000; Rogiers *et al.*, 2006; Famiani *et al.*, 2014), which indicates that 15 - 20 µmol hexose min-1 will accumulate in the number of fruits weighing 1 kg at harvest (hereafter Nberry). Since respiration lies within 15-24 µmol O_2/min/Nberry (recalculated from Kriedemann, 1968; Harris *et al.*, 1970; Koch & Alleweldt, 1978; Terrier *et al.*, 1996), sugars accumulate approximately six times faster than they can be oxidised. In the same way, endogenous malate (0.083 mol/Nberry) can support respiration for 7-11 days at best, or just contribute to the synthesis of approximately one-twentieth of the sugars to be accumulated. Malate decay fits first-order kinetics (Duchêne *et al.*, 2014), and Famiani *et al. (*2014) have confirmed that it can only be a significant respiratory substrate at the very beginning of ripening. Figures such as those above are integral to the understanding of grape metabolism, and they are generated from sequential average samples, which is the commonly accepted way of characterising

berry development. However, gaining fruit dynamics from the one of the population requires the future harvest to be composed of synchronised fruits, which, whatever the stage, seems no longer tenable (Bigard *et al.*, 2019); a fact Coombe (1992) had already anticipated at veraison. Yet, when addressing the more finite features of this process, data on the development of individual berries are still particularly scarce, segmented, or under-interpreted from a kinetic point of view (Lund *et al.*, 2008; Friend *et al.*, 2009; Castellarin *et al.*, 2011; Higginson *et al.*, 2016). Furthermore, the actual velocity of the most elementary metabolic flux in the ripening berry still needs to be established.

In order to approach berry physiology from a strictly quantitative perspective, the flows and timeframes of water, sugar, and malate accumulation in ripening berry are revisited here, based on measurements from thousands of individual fruits, as announced in a preliminary report (Shahood *et al.*, 2019).

MATERIALS AND METHODS

1. Plant material

The *Vitis vinifera* L. cultivars Meunier, Syrah, Zinfandel, and Cabernet-Sauvignon were grown in the experimental vineyard of Montpellier SupAgro during the 2014 and 2015 seasons. The experimental vineyard was planted in 2000 with SO4 as common rootstock. Plants were trained on a double Guyot system at a distance of 1.2 x 2.5 m, under controlled irrigation. The 2015 environmental variables are provided in Supplementary data: Figure S1. Single berry growth (10 berries) was monitored on ML1 microvines, which derived from cv. Meunier (Chaïb *et al.*, 2010; Luchaire *et al.*, 2017) grown in greenhouses with a day/night temperature of 25/15 °C (Rienth *et al.*, 2014). Growing microvines in controlled conditions is convenient for expanding the short period of the year during which veraison and ripening berries can be studied (Torregrosa *et al.*, 2019). Individual diameter changes for Cabernet-Sauvignon and Pinot noir were retrieved from the literature (Friend *et al.*, 2009).

2. Sampling for primary metabolites analyses

Single berries or entire clusters were sampled at different dates. In Experiment 1 (2014), the berry weight and composition were determined for all individual berries from 2-3 clusters sampled at each indicated date (1,035 single berries from cv. Meunier), and on 14 additional whole Meunier clusters, which were respectively pooled, at each indicated date (132 bunches). Clusters were harvested from 19 vines, with a maximum of 30 % clusters sampled.

In Experiment 2 (2015), 696 individual Syrah berries were randomly sampled from 30 vines in order to address fruit heterogeneity within the usual samples representative of the experimental plot, instead of from a few clusters, as in Experiment 1.

In Experiment 3 (2015), synchronised berries were sampled at known durations once their individual softening dates had been determined. For this, 500 berries (cv. Syrah, 3-10 berries per cluster) were tagged with coloured rings according to their individual softening dates (accuracy ± 1 day).

All fruits were weighed and stored at -80 °C within 4 hours of sampling.

3. Monitoring of the volume development of the whole bunch

The growth of 20 clusters cv. Meunier and 5 clusters cv. Zinfandel was monitored without removing them from the vine by weekly immersion, according to Lang & Thorpe (1989). Water loss was determined with a 0.1 g accuracy scale. Berries were counted and weighed at the end of the experiment.

4. Individual berry growth

Berries on ML1 microvine plants were placed in front of a piece of blue cardboard including a surface standard and were periodically photographed with a Nikon Coolpix $L^{-1}10$ 12.1MP digital camera. This contactless procedure eliminates the deformation of flaccid ripe berries as a possible artefact during caliper measurements. Single fruit volume was evaluated from pixel counts using the ImageJ software (http://rsb.info.nih.gov/ij), assuming berries as ellipsoid of revolution. The kinetics of individual Pinot noir and Cabernet-Sauvignon berry diameters was retrieved from Figure 1 and 2 in Friend *et al. (*2009), with the "save xy coordinate" macro in the Image J software, before volume calculation.

5. Sugar and organic acids

Samples were immerged in 5 times their weight of MilliQ water. In order to save the time needed for crushing 2,300 single berries, samples were autoclaved at 120 °C for 5 min, before being homogenised by vigorous shaking.

A preliminary check was carried out to ensure that this procedure did not alter the composition of the berry juices (Supplementary data: Figure S2). HPLC analysis was performed after a second dilution as in Rienth *et al. (*2014).

6. Firmness and colour

Firmness was monitored with a digital penetrometer as in Robin *et al. (*1997), with maximal displacement set to one-tenth of berry diameter. Firmness was inferred from the linear regression of the force data points versus displacement data points. Berry colour (hue angle) was determined with a Minolta CR 200 as in Robin *et al. (*1996).

7. Normalisation of berry volume

The net accumulation of water or solutes per fruit is proportionally affected by genetic variations in the nominal berry volume. Fluxes were thus normalised when adjusting the number of berries investigated according to the cultivar in order to reach an identical fruit weight (1 kg) at maximum growth. For example, 1,000 berries were considered at each sampling date for a cultivar with 1 g berry at maximum volume, 500 berries were considered for a 2 g/berry cultivar, and so on. For the sake of simplicity, density changes during berry ripening (d = 1.04 (green) to d = 1.09 (0.9 mol hexose/kg berry)) were considered negligible.

RESULTS

1. The duration of the second growth phase

1.1. Average berry growth at bunch level

Meunier clusters exhibited the typical double sigmoidal growth patterns, with clearly resolved green growth (Phase I), lag phase (Phase II), and ripening periods (Phase III) (Figure 1). At harvest, the rachis accounted for 3.6 ± 0.8 % of cluster weight only, therefore its contribution was ignored. Noticeably, the average berry volume displayed 1.8-fold variations among clusters (Figure 1a), but all of them fit into comparable double sigmoidal growth curves once the maximal volume had been normalised and a few days adjusted for on the time axis (Figure 1b). The average fruit volume approximatively doubled within 29 ± 2 days, but this duration would be reduced to 20 days if the maximal growth rate observed at the inflexion point were taken into account. The same maximal growth rate was observed in the two successive periods of berry expansion, with a variance lower than 12 %. At the end of ripening, berry volume decreased (shrinking) with noticeable variations among bunches (Figure 1, 2; Supplementary data: Table 1).

1.2. Individual fruits

According to image analysis, single ripening berries from ML1 microvines grown in the greenhouse doubled in volume in 20 days only (Figure 2). Similar growth patterns were recalculated for Pinot noir and Cabernet-Sauvignon, based on previously reported diameter changes (Figure 1, 2 in Friend *et al. (*2009)), irrespective of the considerable variation in fruit size, as related to seed number (Supplementary data: Figure S3,S4, S5).

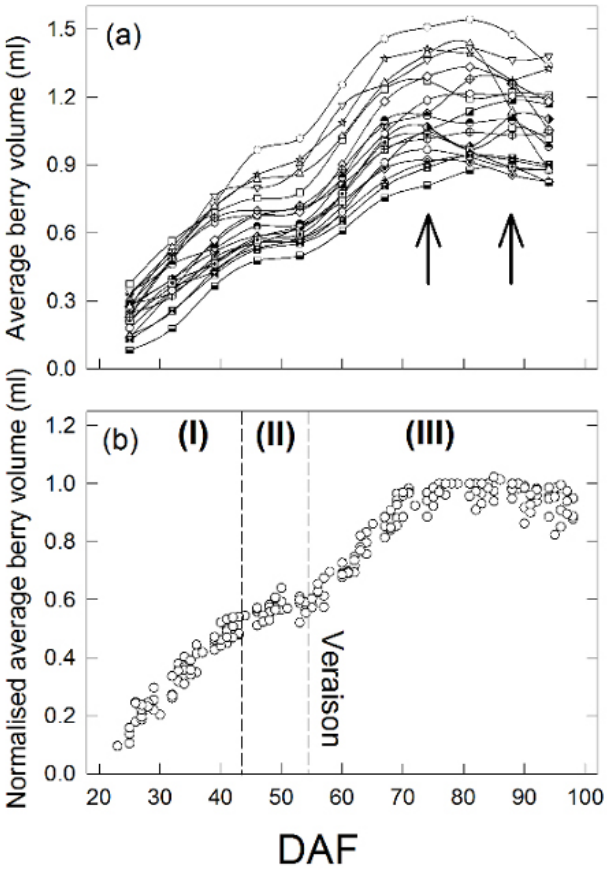

FIGURE 1. Average berry growth in 20 Meunier clusters.

(a) Each curve corresponds to one cluster.

(b) Relative growth following normalisation of the maximal average berry volume and re-synchronisation of the onsets of the second growth period at 55 days after flowering (DAF). Normalised average berry volume: $V/(V_{max} \times Nb)$, where V represents cluster volume, V_{max} represents maximum cluster volume, and Nb represents number of berries per cluster. Arrows correspond to the maximal and minimal time needed to reach maximal volume after mean flowering date (2014-05-15).

(I) Green phase, (II) Lag phase, (III) Ripening phase.

2. Developmental changes in sugar, malate and growth

Meunier bunches harvested simultaneously displayed noticeable discrepancies in average berry weight, sugar and malic acid (Supplementary data: Figure S6). Meunier and Syrah individual berries showed tremendous heterogeneity in weight and composition during the first 20 days of ripening (Figure 3, Figure 4). Even though berry weight was the most variable trait - showing at least 3-fold variations among fruits with the same sugar concentration - the doubling of berry volume described above was still statistically verified during ripening. The sugar/malate relationship was considerably less variable: during the green stage, hexoses increased by up to 0.12 M, mostly in the form of glucose (Supplementary data: Figure S7), until malic acid reached 400 to 600 mEq. It is worth noting that malic acid concentration surpassed 450 mEq in some atypically small berries. Within the same bunches, green and hard berries still accumulating malic acid coexisted with soft berries which contained up to 0.7 M sugars and had lost most of their malic acid (Figure 4).

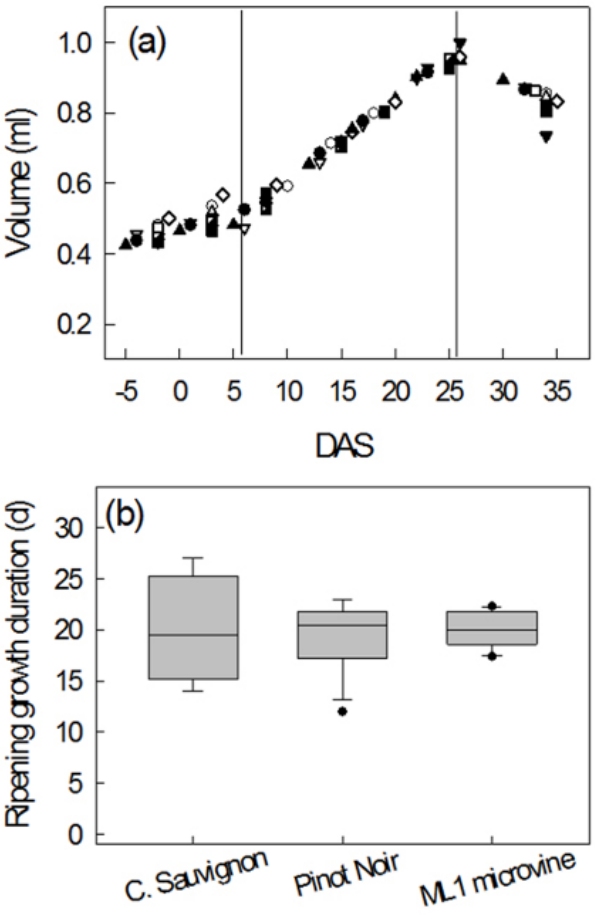

FIGURE 2. Duration of the second growth phase in individual berries.

(a) Growth of 10 single berries on ML1 microvines. Each symbol corresponds to one berry, the diameter of which was measured on successive pictures, before volume calculation and normalisation of the maximum volume. DAS (Days after softening) was normalised by synchronizing the growth curves of all ten berries.

(b) Duration of the second growth phase of ML1 microvine (n = 10), Pinot noir and Cabernet-Sauvignon berries (n = 12). The horizontal line in each box is the median; the top and bottom box edges are the 75th and 25th percentiles; the top and bottom error bars are the 90th and 10th percentiles; and the black dots are outliers at the 95th and 5th percentiles. The three varieties did not exhibit significant differences (ANOVA, $P > 0.05$).

Immediately after softening, massive sugar loading was accompanied by a fast decrease in the Glu/Fru ratio to below 1.6 (Supplementary data: Figure S7). The heterogeneity in sugar concentration among berries within a given cluster diminished above 0.7 M of sugar, with a clear stacking of the "20 days after veraison" samples at 1 M of sugar. However, this tendency could be reversed to more than 40 days after veraison (Figure 4 and inset of Figure 3).

3. Asynchrony in the onset of ripening

Individual Syrah berries were randomly sampled on the experimental plot, yielding similar developmental trends to previous samples devoted to intra-cluster variability, although, as expected, heterogeneity was greater (Figure 4a & 4b). Syrah accumulated 100-150 mEq less malic acid than Meunier before softening, but the sugar/malate relationship exhibited the same slope in both cultivars (Figure 4).

Synchronised berries were sampled at known duration following the determination of their individual softening dates (Figure 4c), which severely limited the heterogeneity in malic acid and sugars compared to previous experiments with undetermined individual softening dates (Figure 4). Delay in the onset of ripening, therefore, appears to be the primary cause of the heterogeneity of individual berries, followed to a lesser extent by possible differences in the speeds of phloem sucrose unloading or malate breakdown.

4. Accumulated sugar versus consumed malate

Berries were ranked according to their total solute concentrations ($mol.L^{-1}$ malate + tartrate + glucose + fructose) as a proxy for vacuolar osmotic pressure. The amount of malic acid and hexoses which had accumulated in each fruit (concentration x volume) was then calculated, and then averaged on successive 0.05 M solute concentration intervals.

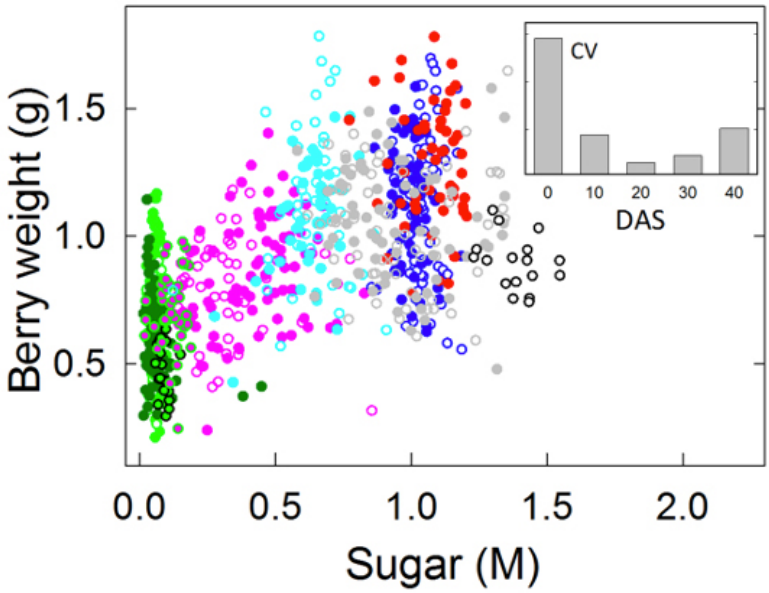

FIGURE 3. The heterogeneity of berry weight along the sugar concentration process in cv. Meunier, cluster-based sampling.

Each point depicts one single berry within one cluster, for which sampling date is indicated by a given colour. -10 DAV (3 clusters: green, dark-green and open-green), 0 DAV (3 clusters: pink open, closed and pink-green boundaries symbols), 10 DAV (2 clusters: cyan open and closed symbols), 20 DAV (2 clusters: blue open and blue closed symbols), 30 DAV (1 cluster: red closed), 40 DAV (2 clusters: grey open and grey closed). Open black circles are the same, cluster averaged shrivelling berries than in Supplementary data: Figure S6. DAV: days after veraison (50 % coloured berries). Inset: coefficient of variation (CV) of sugar concentration with respect to the sampling date.

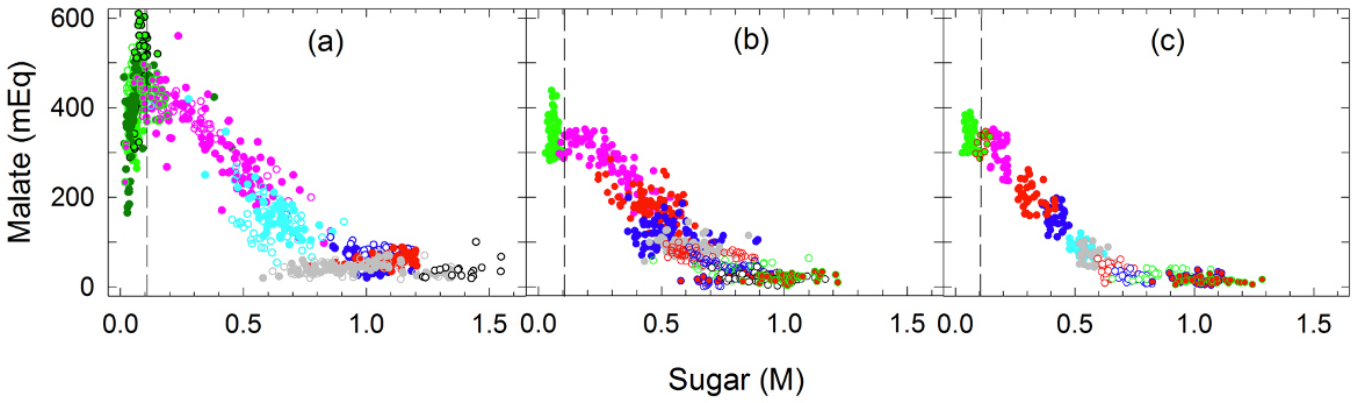

FIGURE 4. Heterogeneity in malate and sugar concentrations in individual berries according to the sampling method.

Softening is indicated by dotted line.

(a) Meunier berries from clusters-based sampling. Cluster sampling date: -10 DAV (3 clusters: green, dark-green and open-green circles), 0 DAV (2 clusters: pink and open pink circles), 10 DAV (2 clusters: cyan and open-cyan circles), 20 DAV (2 clusters: blue and open blue circles), 30 DAV (1 cluster: red circles) and 40 DAV (2 clusters: grey and open grey circles). DAV: days after veraison (50 % soft berries).

(b) Syrah berries, random sampling; each point describes one sampled berry: -10 DAV (green circles), 0 DAV (pink circles), 5 DAV (red circles), 8 DAV (blue circles), 13 DAV (grey circles), 18 DAV (open red circles), 25 DAV (open blue circles), 32 DAV (open green circles), 39 DAV (blue red circles), 46 DAV (open black circles) and 55 DAV (green red circles).

(c) Syrah berries, synchronised (known individual softening date). Each point depicts one sampled berry: -1 day after its own softening date (DAS) (green circles), 0 DAS (pink green circles), 1 DAS (pink circles), 3-5 DAS (red circles), 5-6 DAS (blue circles), 7-8 DAS (cyan circles), 8-11 DAS (grey circles), 16-18 DAS (open red circles), 19-22 DAS (open blue circles), 29-30 DAS (open green circles), 37-38 DAS (blue red circles) and 52-54 DAS (green red circles). Softening dates may vary among berries (not shown).

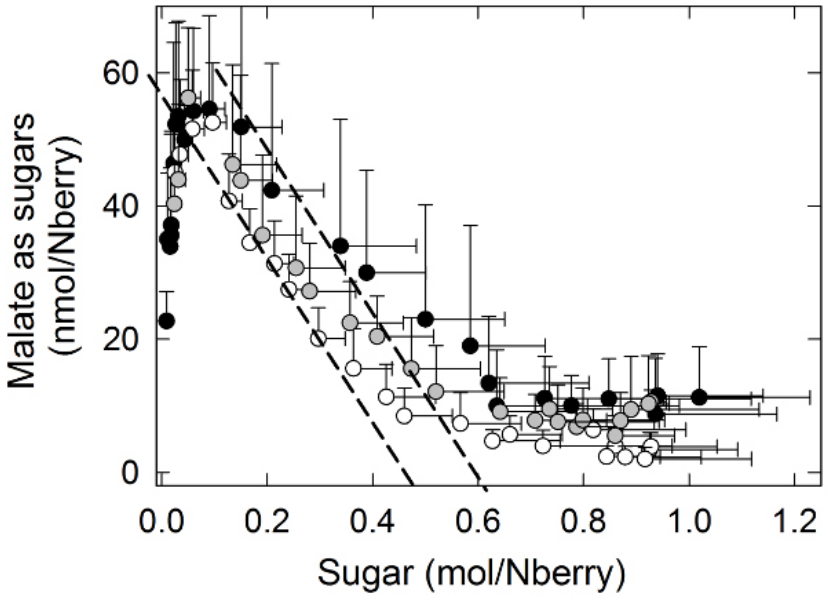

FIGURE 5. Malate breakdown versus accumulated sugar in iso-osmotic berries.

Open circles: Synchronised Syrah berries with known individual softening dates (see Figure 4c). Grey: Syrah berries, random sampling (see Figure 4b). Black: Meunier berries, cluster-based sampling (see Figure 4a). The 2231 individual berries were ranked according to their internal solute concentration (malate + tartrate + glucose + fructose: M + T + S), before calculating malate and sugar content per fruit (concentration x volume) and averaging successive 0.05 M (M + T + S) intervals. Nberry, the number of fruits needed in order to reach 1 kg FW at maximal volume, was 385 for Syrah and 833 for Meunier. In order to check to what extent the neoglucogenic pathway could best contribute to sugar accumulation, malic acid is expressed as sugar equivalent (2 malate/hexose). Dotted lines indicate that, during the first period of ripening, the berry accumulated eight-fold more hexose than possibly formed from malate and that 1 H^+ was consumed per imported sucrose.

Comparable patterns for net malate breakdown versus accumulated hexose were found in the three independent experiments on Syrah or Meunier (Figure 5). Cluster-based sampling noticeably increased the standard deviations compared to random sampling, and synchronised berries yielded the least scattered results. In the first ripening period, 0.25 malic acid disappeared for each accumulated hexose, for both genotypes and sampling conditions. Malate breakdown virtually stopped when around 60 % final hexoses had accumulated. The second phase of sugar loading did not involve further malic acid breakdown.

5. Timeframe for berry ripening

Sequential measurements of colour, firmness, sugars, and pH of individual berries showed that (1) green, hard, acidic (pH 2.7), immature berries, (2) green, soft, acidic post-veraison berries having just started to accumulate sugars, and (3) red or blue soft berries up to the ripe stage were simultaneously present in Cabernet-Sauvignon clusters at the so-called mid-veraison stage (50 % coloured berries) (Figure 6). Firmness decreased at the very beginning of the sugar accumulation process, the few berries found within the 500-1100 gF/mm range indicate that this transition was very fast. Firmness did not exhibit any significant evolution above 0.55 M hexoses, when the first signs of skin colouration appeared. From this point on, noticeable discrepancies appeared in the colouration of the berries at similar sugar concentration, but all berries ended up turning dark blue at 1 M sugar concentration.

Synchronised Syrah berries revealed three successive ripening periods (Figure 7 and 8). First, the net flux of sugar loading in the vacuole was abruptly set at its maximal value (29-43 µmol hexose/min/Nberry) as soon as softening was detected, which is 1.5 to 2 times faster than using usual average samples. Growth resumed six days later (Figure 7 and 8a), followed by a twenty-day period of simultaneous water and sugar accumulation until 0.9 mol hexose/Nberry was reached. Phloem unloading permanently stopped at the end of the second growth phase. Then a third period of relative homeostasis became apparent in the time-averaged samples (Figure 7). However, this representation masks either asynchronised or variable water losses, as illustrated in berries ranked according to total solute concentration (Figure 8a).

DISCUSSION

Present knowledge about berry developmental biology derives essentially from the destructive analysis of sequential random samples taken as "representative". The average population at plot level is implicitly conceived as an ideal berry, whose gene expression and metabolic pathways are modulated by the G x E x M interaction, which has straightforward consequences on wine quality, explaining terroir and millesime effects (Fasoli *et al.*, 2018; Zhu *et al.*, 2019, among many others). However, density sorting (Singleton *et al.*, 1966) has unambiguously showed that this "average" berry is a mixture of developmental stages (Zouid *et al.*, 2013; Carbonell-Bejerano *et al.*, 2016; Friedel *et al.*, 2016; Liu *et al.*, 2016; Bigard *et al.*, 2019). For this reason, some transcriptomic studies stressed the necessity to sort or address fruits separately, in order to elucidate the fine regulation of berry development (Lund *et al.*, 2008; Rienth *et al.*, 2014, 2016; Ghaffari *et al.*, 2020). Obviously, kinetic changes affecting the overall averaged population are equal to fruit ones at single fruit level, only if the delay between berries is negligible (when compared to the duration of the developmental phases to be established). Conversely, we show here that, with a second growth period lasting 20 days at single fruit level, 27-31 days at bunch one and finally 31-39 days at the experimental plot scale (the most conservative durations we could find in the literature (McCarthy, 1999), the time offset between the berries - at the origin of these differences - proves as long as the second growth phase itself.

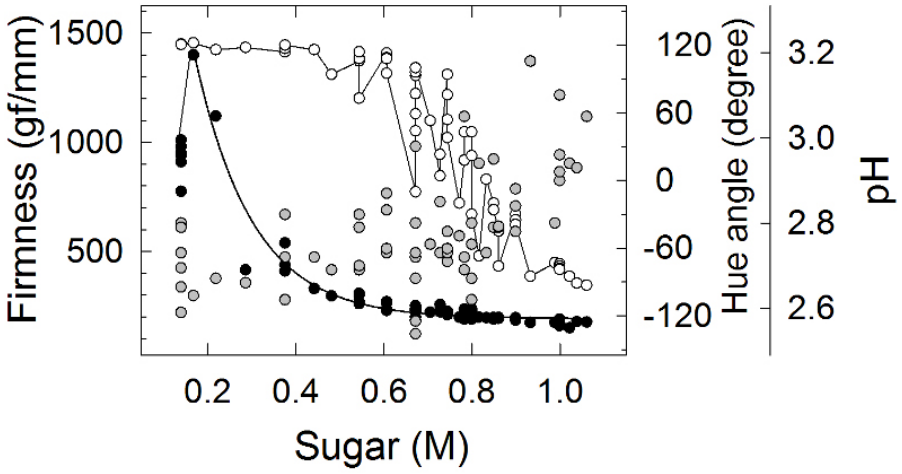

FIGURE 6. Berry heterogeneity in a Cabernet-Sauvignon cluster at mid-veraison (EL 35; Coombe, 1995). Each point corresponds to one berry, successively analysed for firmness (black circles), colour (hue angle: open circles), pH (grey) and sugars (refractometer used for X axes values).

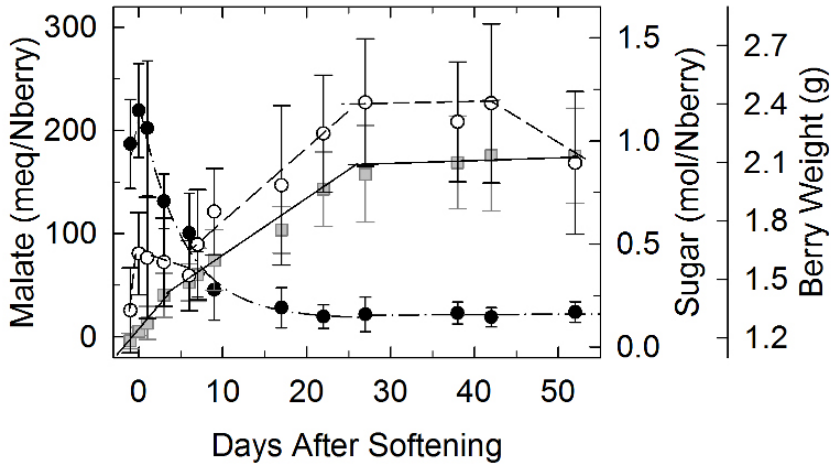

FIGURE 7. Kinetics of malate breakdown (closed circles), sugar loading (grey squares) and berry growth (open circles) in 385 individual Syrah berries (mean ± SD, n = 30) (see Figure 4c).

Moreover, when synchronised, sequential averaged samples of Syrah berries exhibited the same phase III duration (20 days) as continuous monitoring of single berries of Pinot ML1, Meunier, and Cabernet-Sauvignon, which was also compatible with the maximal growth rate observed for clusters of Meunier or Zinfandel (Supplementary data: Figure S4; S8). Although further work is needed to generalise such a duration within a wider range of genotypes and experimental conditions, the reproducible three-week growth period suggests that the kinetic changes observed in the literature may primarily reflect the variable temporal spread of berry cohorts in different sites, rather than the variations in individual ripening speeds.

In this respect, a time lag of three weeks between berries has already been documented based on loss of firmness or colouring data, without having drawn the kinetic consequences from it (Robin *et al.*, 1997; Vondras *et al.*, 2016). Preliminary observations indicated that the offset between clusters should be first attributed to their respective flowering dates (Supplementary data: Figure S8).

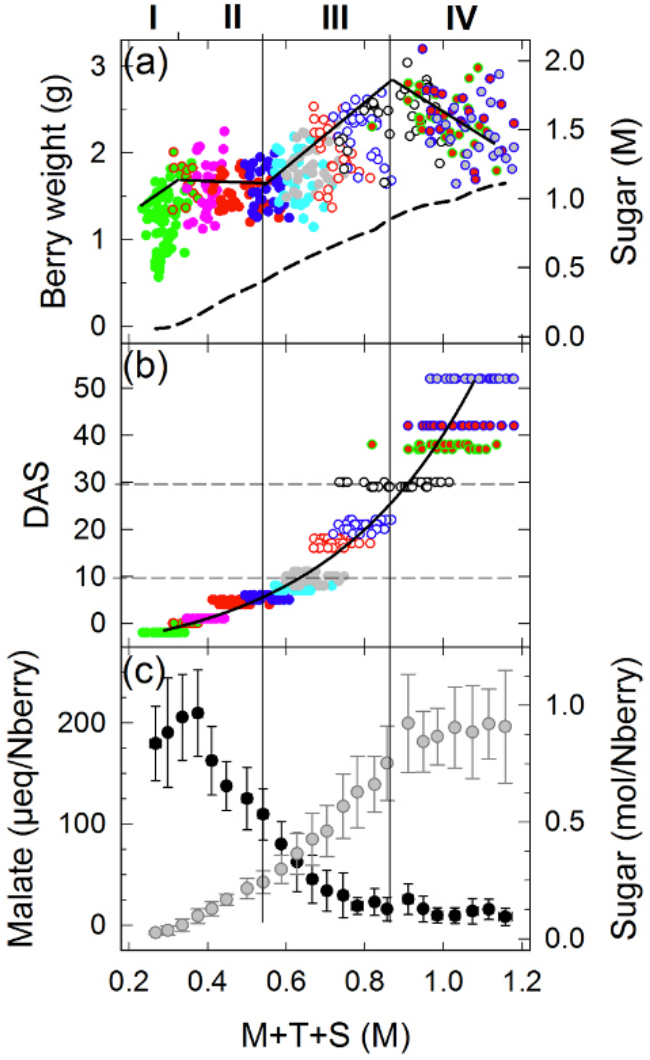

FIGURE 8. Development of Syrah berries with respect to their own vacuolar solute concentration as a proxy for osmotic pressure.

(a) Single berry weight; each colour refers to days after softening (DAS) as indicated in (b). Black line: average berry weight; dotted line: sugar concentration.

(b) Days after softening (DAS); black line: exponential fit.

(c) Average malate (black) and sugar (grey) contents of 385 fruits, corresponding to 1 kg FW at the completion of their growth period. Means (±SD) were calculated at successive 0.05 M (M+T+S) intervals (from 9 to 26 berries, 16 on average).

New developmental phases: (I) Green stage (asynchronised hard berries), (II) Soft berries accumulating sugars at constant volume, (III) Ripening growth period (III-IV transition); Arrest of phloem unloading, and (IV) Berry shriveling. M + T + S: malate + tartrate + glucose + fructose.

Addressing the individual berry entails a change in paradigm in terms of its internal clock. At first, the key events associated with ripening, which were previously thought to be simultaneous, appeared to be sequential. Up to 0.12 M hexoses, principally glucose, slowly accumulates together with 0.25 M malate in hard, green fruits as already described (Houel *et al.*, 2015; Rienth *et al.*, 2016). Changes in firmness occurred concomitantly with the sudden acceleration of sugar storage. Intense transcriptomic changes controlling diverse cell-wall proteins and key transporters, such as the vacuolar hexose/H^+ antiporter *VviHT6* (EST RB004G11 in Terrier *et al.*, 2005), amongst other ripening related genes, were actually detected as soon as softening occurred, before any changes in sugar, colouration or malic acid could be measured (Rienth *et al.*, 2016). Changes in colour occurred later (0.6 M hexoses) in Cabernet-Sauvignon, as it did in Zinfandel and Pinot noir (Castellarin *et al.*, 2016; Vondras *et al.*, 2016; Bigard *et al.*, 2019). In addition, the hue angle illustrated a plasticity of anthocyanin synthesis in the sub-epidermal tissue versus sugar accumulation in the flesh, possibly related to variations in berry microenvironment or seed number (Reshef *et al.*, 2017; Sun *et al.*, 2017). Therefore, colouration does not seem to be the best indicator for the advancement of ripening, so sugar and water fluxes which have been calculated from visually-sorted berries must be considered with circumspection (Lücker *et al.*, 2009; Gouthu *et al.*, 2014; Zhang & Keller, 2017). Synchronised samples allowed the timings of berry growth, sugar loading and malate breakdown to be deciphered with unprecedented precision, whenever the metabolic fluxes calculated from these data remain scrambled by the marked heterogeneity in berry volume; hence the necessity to sort and average a large number of fruits. We can establish here that a reference pericarp volume displays quite invariant growth kinetics: fluxes in genotypes showing two-fold differences in nominal berry sizes were convincingly standardised when taking into account the development of the (cultivar adjusted) number of berries reaching 1 kg at maximal growth. The dramatic heterogeneity in sugar and malate concentrations among individual fruits harvested simultaneously was essentially explained by delayed softening dates, not changing ripening speeds. A considerable osmotic gradient thus exists between neighbouring berries, which should result in water flow from pre-veraison to ripening berries, in exactly the same way as leaves when their hydric potential falls below -0.8 MPa (Greenspan *et al.*, 1994). However, the expected siphoning of water by ripening berries is prevented by delayed growth until major solutes reach around 0.6 M, thus facilitating the completion of the first growth period in late pre-veraison fruits. Non-destructive firmness and diameter measurements on the same berry have already led Coombe & Bishop (1980) and Coombe & Phillips (1982) to propose that growth resumes six days after softening, in line with the delay following the activation of sugar loading observed in the

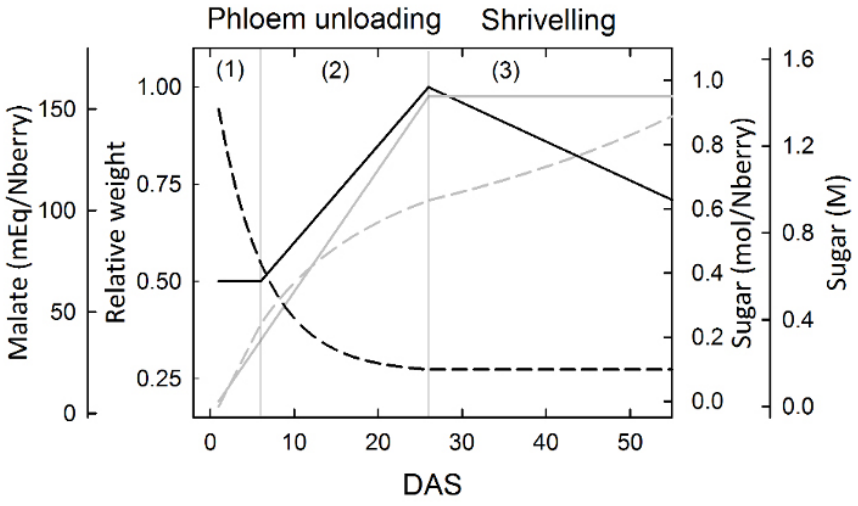

FIGURE 9. Minimal model of berry ripening.

DAS: Days After Softening. Phase (1): full activation of sugar loading & malate breakdown, no expansion. Phase (2): full-rate sugar & water loading; (2a) malate breakdown (2b) completion of malate breakdown. Phase (3): water and sugar import blocked, evaporation. Sugar content per berry (grey line), sugar concentration (dashed grey line), growth (black line), and malate content per berry (dashed black line). Results were normalised for the number of berries that weighed 1 kg (Nberry) at the completion of phloem unloading (phase 2-phase 3 transition).

present study. Water in phloem mass flow must thus be exported until skin extensibility increases (Huang & Huang, 2001); therefore, xylem back-flow (Zhang & Keller, 2017) should be maximal during the first week of ripening.

After softening, the time required by each individual berry to reach the measured concentrations was fitted to an exponential model, making it possible to re-synchronise thousands of berries whose individual softening dates could not be reasonably measured (Figure 8, Supplementary data: Figure S9, S10). Growth patterns remained compatible with synchronised Syrah samples, even though erratic 1.8-fold variations in mean berry weight per cluster induced a higher bias in the case of Meunier, because of non-random sampling. While the usual, average samples representative of the experimental plot will typically provide an accumulation rate of 17 µmol hexose/min/Nberry within 49 days (Supplementary data: Figure S11; Supplementary data: Table S2), synchronised ones just need 26 days to reach 0.9 mol hexose/Nberry (approximately 10 % probable alcohol), after which phloem unloading definitively stops. Further gain in concentration relies on berry shrivelling (Figures 8 and 10; Supplementary data: Figure S6a) - as discussed by McCarthy (1999) - on what appears to be a quite well-synchronised berry population. Constant hexose accumulation at 24 µmol/min/Nberry for 26 days appears to be the simplest model; however, sudden activation of up to 43 µmol/min/Nberry followed by minor decay is also plausible (Figures 7 and 9). The timeframe observed from the destructive analysis of synchronised berries noticeably fits the 6-day delay between softening and growth resumption as discussed above, followed by a 20-day expansion period, as recalculated from non-destructive measurements on single fruits. It must be underlined that sugar loading at a constant rate in an expanding volume arithmetically implies a slowing down of the daily increment in concentration (Figure 9). Such a slowdown does not mean that late berries "ripen faster" than the first ones (Gouthu *et al.*, 2014). Moreover, present data do not confirm that sugar unloading might continue after growth cessation (McCarthy & Coombe, 1999; Keller *et al.*, 2015). This specific question requires further work, since the averaging of late berries which are still growing and accumulating sugars with advanced ones just losing water after the cessation of phloem unloading may have been interpreted as accumulation of sugars at constant volume (Supplementary data: Figure S12).

Malate breakdown is delayed from the onset of sugar accumulation under exceptionally low temperatures (Rienth *et al.*, 2016), but none of the thousand berries analysed here escaped an almost immediate initiation of malic acid breakdown at the outset of hexose accumulation. Malate can be a substrate for gluconeogenesis (2 malate + 4 $H^+ \rightarrow$ 1 hexose + 2 CO_2),

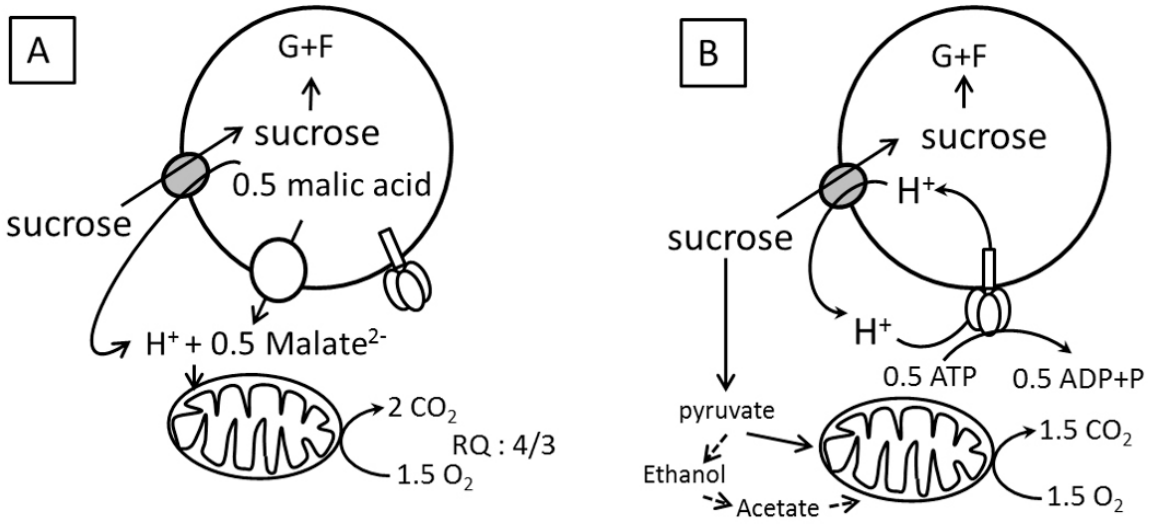

FIGURE 10. Shift in the energisation of sugar transport in the vacuole of ripening berries.

(a) At the onset of ripening, the discharge of vacuolar malate electrically balances a proton/sugar exchange, and malic acid is respired when released into the cytoplasm. This prevents cytoplasmic acidosis. Following the exhaustion of vacuolar malic acid (b), electro-neutralisation requires protons exchanged with sugar to now be pumped back into the vacuole, which consumes ATP. Respiration shifts from malic acid to sugars and aereobic fermentative pathway is induced.

respiration ($2\,H^+ + Malate + 3\,O_2 \rightarrow 4\,CO_2 + 3\,H_2O$), or fermentation ($Malate + 2\,H^+ \rightarrow Ethanol + 2\,CO_2$) (Ruffner & Hawker, 1977; Ruffner, 1982a; Ruffner, 1982b; Terrier & Romieu, 2001; Sweetman *et al.*, 2009; Famiani *et al.*, 2014). The continuation of sugar accumulation above 0.7 mol/Nberry, following the arrest of malate breakdown, clearly confirms that there is no strict need for malic acid release from the vacuole for sugar import. The initial velocity of malate breakdown reached 8 µmol/min/Nberry in synchronised berries, four times faster than inferred from random samples in the literature (1.9 ± 0.2 µmol/min/Nberry) (Supplementary data: Figure S13, Table S3). Therefore, the possible contribution of malate to respiration (24 µmol O_2/min/Nberry) remarkably matches the O_2 demand of the ripening fruit (Harris *et al.*, 1970; Koch & Alleweldt, 1978; Terrier *et al.*, 1996). That malate actually becomes the major respiratory substrate at the onset of ripening could not be ascertained on asynchronised fruit samples (Famiani *et al.*, 2014). P/O measurements on grape mitochondria oxidising malate (Romieu *et al.*, 1992) indicated that 5 ATP would be produced per O_2 reduced, thus 0.2-0.3 hexoses should be imported during the regeneration of one ATP by oxidative phosphorylation. Sucrose may be released from vascular parenchyma cell to berry apoplast through energy silent SWEET facilitators (Milne *et al.*, 2018). Subsequent hydrolysis bycell-wall invertase, followed byhexose/H^+ symport towards the plasma membrane of the pericarp cell, would recruit more than 25 % cellular ATP, notwithstanding ATP needed for terminal vacuolar transport. In this respect, the global 0.5 H^+/hexose exchange described here seems consistent with the transcriptional activation of the *vviHT6* gene (*VIT_18s0122g00850*; EST RB004G11: Rienth *et al.*, 2016; Terrier *et al.*, 2005) and the accumulation of the corresponding peptide on the tonoplast membrane (Kuang *et al.*, 2019), sucrose being preferentially transported by *AtTMT1/2*, the *VviHT6* ortholog in *Arabidopsis* (Schulz *et al.*, 2011). The 10^5 H^+ gradient at the onset of ripening would then drain most cytoplasmic sucrose from the vacuole, concomitantly with a ten-fold activation of the *VviSPS1* transcript (Sucrose Phosphate Synthase), suggesting that intense sucrose synthesis may suddenly take place in the cytoplasm (Rienth *et al.*, 2016; Sarry *et al.*, 2004). At first, the exchange of H^+ for sucrose is electrically balanced with the exit of the anion malate, and acidity is detoxified in the cytoplasm by malic acid respiration. Above 0.7 M sugars, malate is no longer available for charge compensation, therefore H^+ exchanged with sucrose must be pumped back into the less, but still acidic, vacuole, which is in line with the large activation of V-ATPase and H^+-PPiase during late-ripening (Terrier *et al.*, 2001) (Figure 10). The energy balance of the berries may thus be impaired following the arrest of malate breakdown, hence their propensity to aerobic fermentation (Tesnière *et al.*, 1994). Transcriptomic changes accompanying the arrest of phloem unloading in single berries will be presented in a subsequent paper (Savoi *et al.*, in preparation).

CONCLUSION

The present revisit of basic metabolic flux in the berry provides a faithful, quantitative, and time-resolved framework for fruit ripening, surpassing the composite nature of previous developmental stages. Phloem sucrose unloading is activated at full rate for a 26-day period, after which it suddenly stops. Berry growth is inhibited during the first 6 days of intense phloem unloading, but both water and sugar accumulation stop simultaneously at the end of the process. An overall vacuolar sucrose/H^+ exchange, electro-neutralised with malate, sheds light on the long-standing question of the sugar/acidity interplay in grapevine. As well as metabolism, the temporal structure of berry cohorts emerges as a novel possible regulatory site in terms of the impact of GxE interaction on oenological attributes. Process-based models should, therefore, consider both these basically different mechanisms, each acting at fruit and population levels. The present work also highlights the sampling strategy as a critical bottleneck of time resolution in studies on omics. High throughput non-destructive real-time monitoring of single berry development is needed to improve the present model of berry ripening, which overlooks the impact of berry microenvironment on its own hydric balance and primary metabolism.

ACKNOWLEDGEMENTS

RS was supported by a PhD grant from the ministry of higher education (Damascus, Syria). The authors warmly thank Dr. Philippe Chatelet for his useful suggestions regarding text editing.

REFERENCES

Afoufa-Bastien, D., Medici, A., Jeauffre, J., Coutos-Thévenot, P., Lemoine, R., Atanassova, R., & Laloi, M. (2010). The *Vitis vinifera* sugar transporter gene family: Phylogenetic overview and macroarray expression profiling. *BMC Plant Biology*, *10*(1), 245. https://doi.org/10.1186/1471-2229-10-245

Bigard, A., Romieu, C., Sire, Y., Veyret, M., Ojéda, H., & Torregrosa, L. (2019). The kinetics of grape ripening revisited through berry density sorting. *OENO One*, *53*(4). https://doi.org/10.20870/oeno-one.2019.53.4.2224

Burzynski-Chang, E. A., Brown, E. J., Reshef, N., & Sacks, G. L. (2020). Malate content in wild *Vitis* spp. Demonstrates a range of behaviors during berry maturation. *American Journal of Enology and Viticulture*, *71*(1), 80–87. https://doi.org/10.5344/ajev.2019.19015

Carbonell-Bejerano, P., Rodríguez, V., Hernáiz, S., Royo, C., Dal Santo, S., Pezzotti, M., & Martínez-Zapater, J. M. (2016). Reducing sampling bias in molecular studies of grapevine fruit ripening: Transcriptomic assessment of the density sorting method. *Theoretical and Experimental Plant Physiology*, *28*(1), 109–129. https://doi.org/10.1007/s40626-016-0059-5

Castellarin, S. D., Gambetta, G. A., Wada, H., Krasnow, M. N., Cramer, G. R., Peterlunger, E., Shackel, K. A., & Matthews, M. A. (2016). Characterization of major ripening events during softening in grape: Turgor, sugar accumulation, abscisic acid metabolism, colour development, and their relationship with growth. *Journal of Experimental Botany*, *67*(3), 709–722. https://doi.org/10.1093/jxb/erv483

Castellarin, S. D., Gambetta, G. A., Wada, H., Shackel, K. A., & Matthews, M. A. (2011). Fruit ripening in *Vitis vinifera*: Spatiotemporal relationships among turgor, sugar accumulation, and anthocyanin biosynthesis. *Journal of Experimental Botany*, *62*(12), 4345–4354. https://doi.org/10.1093/jxb/err150

Chaïb, J., Torregrosa, L., Mackenzie, D., Corena, P., Bouquet, A., & Thomas, M. R. (2010). The grape microvine – a model system for rapid forward and reverse genetics of grapevines. *The Plant Journal*, *62*(6), 1083–1092. https://doi.org/10.1111/j.1365-313X.2010.04219.x

Coombe, B. G. (1987). Distribution of solutes within the developing grape berry in relation to its morphology. *American Journal of Enology and Viticulture*, *38*(2), 120–127.

Coombe, B. G. (1992). Research on development and ripening of the grape berry. *American Journal of Enology and Viticulture*, *43*(1), 101–110.

Coombe, B. g. (1995). Growth stages of the grapevine: Adoption of a system for identifying grapevine growth stages. *Australian Journal of Grape and Wine Research*, *1*(2), 104–110. https://doi.org/10.1111/j.1755-0238.1995.tb00086.x

Coombe, B. G., & Bishop, G. R. (1980). Development of the grape berry. II. Changes in diameter and deformability during veraison. *Australian Journal of Agricultural Research*, *31*(3), 499–509. https://doi.org/10.1071/ar9800499

Coombe, B. G., & McCarthy, M. G. (2000). Dynamics of grape berry growth and physiology of ripening. *Australian Journal of Grape and Wine Research*, *6*(2), 131–135. https://doi.org/10.1111/j.1755-0238.2000.tb00171.x

Coombe, B. G., & Phillips, P. E. (1982). Development of the grape berry. III. Compositional changes during veraison measured by sequential hypodermic sampling. *Proceedings of the UCD Grape and Wine Centennial Symposium*, 132–136.

Davies, C., & Robinson, S. P. (1996). Sugar accumulation in grape berries (cloning of two putative vacuolar invertase cdnas and their expression in grapevine tissues). *Plant Physiology*, *111*(1), 275–283. https://doi.org/10.1104/pp.111.1.275

Diakou, P., Moing, A., Svanella, L., Ollat, N., Rolin, D. B., Gaudillere, M., & Gaudillere, J. P. (1997). Biochemical comparison of two grape varieties differing in juice acidity. *Australian Journal of Grape and Wine Research*, *3*(3), 1–10. https://doi.org/10.1111/j.1755-0238.1997.tb00122.x

Duchêne, E., Dumas, V., Jaegli, N., & Merdinoglu, D. (2014). Genetic variability of descriptors for grapevine berry acidity in Riesling, Gewürztraminer and their progeny. *Australian Journal of Grape and Wine Research*, *20*(1), 91–99. https://doi.org/10.1111/ajgw.12051

Famiani, F., Farinelli, D., Palliotti, A., Moscatello, S., Battistelli, A., & Walker, R. P. (2014). Is stored malate the quantitatively most important substrate utilised by respiration and ethanolic fermentation in grape berry pericarp during ripening? *Plant Physiology and Biochemistry*, *76*, 52–57. https://doi.org/10.1016/j.plaphy.2013.12.017

Fasoli, M., Richter, C. L., Zenoni, S., Bertini, E., Vitulo, N., Santo, S. D., Dokoozlian, N., Pezzotti, M., & Tornielli, G. B. (2018). Timing and order of the molecular events marking the onset of berry ripening in grapevine. *Plant Physiology*, *178*(3), 1187–1206. https://doi.org/10.1104/pp.18.00559

Friedel, M., Sorrentino, V., Blank, M., & Schüttler, A. (2016). Influence of berry diameter and colour on some determinants of wine composition of *Vitis vinifera* L. cv. Riesling. *Australian Journal of Grape and Wine Research*, *22*(2), 215–225. https://doi.org/10.1111/ajgw.12210

Friend, A. P., Trought, M. C. T., & Creasy, G. L. (2009). The influence of seed weight on the development and growth of berries and live green ovaries in *Vitis vinifera* L. cvs. Pinot noir and Cabernet-Sauvignon. *Australian Journal of Grape and Wine Research*, *15*(2), 166–174. https://doi.org/10.1111/j.1755-0238.2009.00050.x

Ghaffari, S., Reynard, J. S., & Rienth, M. (2020). Single berry reconstitution prior to RNA-sequencing reveals novel insights into transcriptomic remodeling by leafroll virus infections in grapevines. *Scientific Reports*, 10(1), 12905. https://doi.org/10.1038/s41598-020-69779-1

Gambetta, G. A., Matthews, M. A., Shaghasi, T. H., McElrone, A. J., & Castellarin, S. D. (2010). Sugar and abscisic acid signaling orthologs are activated at the onset of ripening in grape. *Planta*, *232*(1), 219–234. https://doi.org/10.1007/s00425-010-1165-2

Gouthu, S., O'Neil, S. T., Di, Y., Ansarolia, M., Megraw, M., & Deluc, L. G. (2014). A comparative study of ripening among berries of the grape cluster reveals an altered transcriptional programme and enhanced ripening rate in delayed berries. *Journal of Experimental Botany*, *65*(20), 5889–5902. https://doi.org/10.1093/jxb/eru329

Greenspan, M. D., Shackel, K. A., & Matthews, M. A. (1994). Developmental changes in the diurnal water budget of the grape berry exposed to water deficits. *Plant, Cell & Environment*, *17*(7), 811–820. https://doi.org/10.1111/j.1365-3040.1994.tb00175.x

Harris, J. M., Kriedemann, P. E., & Possingham, J. V. (1970). Grape berry respiration: Effects of metabolic inhibitors. *VITIS - Journal of Grapevine Research*, *9*(4), 291–291. https://doi.org/10.5073/vitis.1970.9.291-298

Higginson, E. G., Lloyd, N. D. R., Kravchuk, O., Ford, C. M., & Thomas, M. R. (2016). A high-throughput UHPLC MS/MS method for evaluation of tartaric and malic acid concentration in individual grapevine berries. *Australian Journal of Grape and Wine Research*, *22*(1), 16–23. https://doi.org/10.1111/ajgw.12170

Houel, C., Chatbanyong, R., Doligez, A., Rienth, M., Foria, S., Luchaire, N., Roux, C., Adivèze, A., Lopez, G., Farnos, M., Pellegrino, A., This, P., Romieu, C., & Torregrosa, L. (2015). Identification of stable QTLs for vegetative and reproductive traits in the microvine (*Vitis vinifera* L.) using the 18 K Infinium chip. *BMC Plant Biology*, *15*, 205. https://doi.org/10.1186/s12870-015-0588-0

Huang, X.-M., & Huang, H.-B. (2001). Early post-veraison growth in grapes: Evidence for a two-step mode of berry enlargement. *Australian Journal of Grape and Wine Research*, *7*(3), 132–136. https://doi.org/10.1111/j.1755-0238.2001.tb00200.x

Keller, M., & Shrestha, P. M. (2014). Solute accumulation differs in the vacuoles and apoplast of ripening grape berries. *Planta*, *239*(3), 633–642. https://doi.org/10.1007/s00425-013-2004-z

Keller, M., Zhang, Y., Shrestha, P. M., Biondi, M., & Bondada, B. R. (2015). Sugar demand of ripening grape berries leads to recycling of surplus phloem water via the xylem. *Plant, Cell & Environment*, *38*(6), 1048–1059. https://doi.org/10.1111/pce.12465

Koch, R., & Alleweldt, G. (1978). Der gaswechsel reifender weinbeeren. *VITIS - Journal of Grapevine Research*, *17*(1), 30–44. https://doi.org/10.5073/vitis.1978.17.30-44

Kriedemann, P. E. (1968). Observations on gas exchange in the developing sultana berry. *Australian Journal of Biological Sciences*, *21*(5), 907–916. https://doi.org/10.1071/bi9680907

Kuang, L., Chen, S., Guo, Y., & Ma, H. (2019). Quantitative proteome analysis reveals changes in the protein landscape during grape berry development with a focus on vacuolar transport proteins. *Frontiers in Plant Science*, *10*. https://doi.org/10.3389/fpls.2019.00641

Lang, A., & Thorpe, M. R. (1989). Xylem, phloem and transpiration flows in a grape: Application of a technique for measuring the volume of attached fruits to high resolution using Archimedes' principle. *Journal of Experimental Botany*, *40*(10), 1069–1078. https://doi.org/10.1093/jxb/40.10.1069

Lecourieux, F., Lecourieux, D., Vignault, C., & Delrot, S. (2010). A sugar-inducible protein kinase, VvSK1, regulates hexose transport and sugar accumulation in grapevine cells. *Plant Physiology*, *152*(2), 1096–1106. https://doi.org/10.1104/pp.109.149138

Liu, X., Li, J., Tian, Y., Liao, M., & Zhang, Z. (2016). Influence of berry heterogeneity on phenolics and antioxidant activity of grapes and wines: A primary study of the new winegrape cultivar Meili (*Vitis vinifera* L.). *PLoS ONE*, *11*(3). https://doi.org/10.1371/journal.pone.0151276

Luchaire, N., Rienth, M., Romieu, C., Nehe, A., Chatbanyong, R., Houel, C., Ageorges, A., Gibon, Y., Turc, O., Muller, B., Torregrosa, L., & Pellegrino, A. (2017). Microvine: A new model to study grapevine growth and developmental patterns and their responses to elevated temperature. *American Journal of Enology and Viticulture*, *68*(3), 283–292. https://doi.org/10.5344/ajev.2017.16066

Lücker, J., Laszczak, M., Smith, D., & Lund, S. T. (2009). Generation of a predicted protein database from EST data and application to iTRAQ analyses in grape (*Vitis vinifera* cv. Cabernet-Sauvignon) berries at ripening initiation. *BMC Genomics*, *10*(1), 50. https://doi.org/10.1186/1471-2164-10-50

Lund, S. T., Peng, F. Y., Nayar, T., Reid, K. E., & Schlosser, J. (2008). Gene expression analyses in individual grape (*Vitis vinifera* L.) berries during ripening initiation reveal that pigmentation intensity is a valid indicator of developmental staging within the cluster. *Plant Molecular Biology*, *68*(3), 301–315. https://doi.org/10.1007/s11103-008-9371-z

Matthews, M. A., Cheng, G., & Weinbaum, S. A. (1987). Changes in water potential and dermal extensibility during grape berry development. *Journal of the American Society for Horticultural Science (USA)*.

Matthews, M. A., Thomas, T. R., & Shackel, K. A. (2009). Fruit ripening in *Vitis vinifera* L.: Possible relation of veraison to turgor and berry softening. *Australian Journal of Grape and Wine Research*, 15(3), 278–283. https://doi.org/10.1111/j.1755-0238.2009.00060.x

McCarthy, M. G. (1999). Weight loss from ripening berries of Shiraz grapevines (*Vitis vinifera* L. cv. Shiraz). *Australian Journal of Grape and Wine Research*, *5*(1), 10–16. https://doi.org/10.1111/j.1755-0238.1999.tb00145.x

McCarthy, M. G., & Coombe, B. G. (1999). Is weight loss in ripening grape berries cv. Shiraz caused by impeded phloem transport? *Australian Journal of Grape and Wine Research*, *5*(1), 17–21. https://doi.org/10.1111/j.1755-0238.1999.tb00146.x

Milne, R. J., Grof, C. P., & Patrick, J. W. (2018). Mechanisms of phloem unloading: Shaped by cellular pathways, their conductances and sink function. *Current Opinion in Plant Biology*, *43*, 8–15. https://doi.org/10.1016/j.pbi.2017.11.003

Nieves-Cordones, M., Andrianteranagna, M., Cuéllar, T., Chérel, I., Gibrat, R., Boeglin, M., Moreau, B., Paris, N., Verdeil, J.-L., Zimmermann, S., & Gaillard, I. (2019). Characterization of the grapevine Shaker K+ channel VvK3.1 supports its function in massive potassium fluxes necessary for berry potassium loading and pulvinus-actuated leaf movements. *New Phytologist*, 222(1), 286–300. https://doi.org/10.1111/nph.15604

Ollat, N., & Gaudillere, J. P. (1998). The effect of limiting leaf area during stage I of berry growth on development and composition of berries of *Vitis vinifera* L. cv. Cabernet-Sauvignon. *American Journal of Enology and Viticulture*, *49*(3), 251–258.

Reshef, N., Walbaum, N., Agam, N., & Fait, A. (2017). Sunlight modulates fruit metabolic profile and shapes the spatial pattern of compound accumulation within the grape cluster. *Frontiers in Plant Science*, *8*. https://doi.org/10.3389/fpls.2017.00070

Rienth, M., Torregrosa, L., Luchaire, N., Chatbanyong, R., Lecourieux, D., Kelly, M. T., & Romieu, C. (2014). Day and night heat stress trigger different transcriptomic responses in green and ripening grapevine (*Vitis vinifera*) fruit. *BMC Plant Biology*, *14*, 108. https://doi.org/10.1186/1471-2229-14-108

Rienth, M., Torregrosa, L., Sarah, G., Ardisson, M., Brillouet, J.-M., & Romieu, C. (2016). Temperature desynchronizes sugar and organic acid metabolism in ripening grapevine fruits and remodels their transcriptome. *BMC Plant Biology*, *16*, 164. https://doi.org/10.1186/s12870-016-0850-0

Robin, J. P., Abbal, P., & Flanzy, C. (1996). La fermeté des baies de raisin: Définition d' un indice de fermeté, corrélation avec les modifications de couleur et application à la détection précoce de la veraison. *Oenologie 95: 5e. Symposium International d' Oenologie*, 19–114.

Robin, J. P., Abbal, P., & Salmon, J. M. (1997). Fermeté et maturation du raisin. Définition et évolution de différents paramètres rhéologiques au cours de la maturation. *Journal International des Sciences de la Vigne et du Vin, 31*(3), 127–138.

Rogiers, S. Y., Greer, D. H., Hatfield, J. M., Orchard, B. A., & Keller, M. (2006). Solute transport into Shiraz berries during development and late-ripening shrinkage. *American Journal of Enology and Viticulture*, *57*(1), 73–80.

Romieu, C., Tesniere, C., Than-Ham, L., Flanzy, C., & Robin, J.-P. (1992). An examination of the importance of anaerobiosis and ethanol in causing injury to grape mitochondria. *American Journal of Enology and Viticulture*, *43*(2), 129–133.

Ruffner, H. P. (1982a). Metabolism of tartaric and malic acids in Vitis: A review—Part A. *VITIS - Journal of Grapevine Research*, *21*(3), 247–247. https://doi.org/10.5073/vitis.1982.21.247-259

Ruffner, H. P. (1982b). Metabolism of tartaric and malic acids in Vitis: A review—Part B. *VITIS - Journal of Grapevine Research*, *21*(4), 346–346. https://doi.org/10.5073/vitis.1982.21.345-358

Ruffner, H. P., & Hawker, J. S. (1977). Control of glycolysis in ripening berries of *Vitis vinifera*. *Phytochemistry*, *16*(8), 1171–1175. https://doi.org/10.1016/S0031-9422(00)94354-1

Sarry, J.-E., Sommerer, N., Sauvage, F.-X., Bergoin, A., Rossignol, M., Albagnac, G., & Romieu, C. (2004). Grape berry biochemistry revisited upon proteomic analysis of the mesocarp. *PROTEOMICS*, *4*(1), 201–215. https://doi.org/10.1002/pmic.200300499

Schulz, A., Beyhl, D., Marten, I., Wormit, A., Neuhaus, E., Poschet, G., Büttner, M., Schneider, S., Sauer, N., & Hedrich, R. (2011). Proton-driven sucrose symport and antiport are provided by the vacuolar transporters SUC4 and TMT1/2. *The Plant Journal*, *68*(1), 129–136. https://doi.org/10.1111/j.1365-313X.2011.04672.x

Shahood, R., Savoi, S., Bigard, A., Torregrosa, L., & Romieu, C. (2019). From average to individual berry, a paradigm shift for accurate analysis of water and primary metabolites accumulation into grapevine fruit. Proceedings of the 21st International Symposium GiESCO, Thessaloniki, 24–28 June 2019, pp. 354–358.

Singleton, V. L., Ough, C. S., & Nelson, K. E. (1966). Density separations of wine grape berries and ripeness distribution. *American Journal of Enology and Viticulture*, *17*(2), 95–105.

Sun, R.-Z., Cheng, G., Li, Q., He, Y.-N., Wang, Y., Lan, Y.-B., Li, S.-Y., Zhu, Y.-R., Song, W.-F., Zhang, X., Cui, X.-D., Chen, W., & Wang, J. (2017). Light-induced Variation in Phenolic Compounds in Cabernet-Sauvignon Grapes (*Vitis vinifera* L.) Involves Extensive Transcriptome Reprogramming of Biosynthetic Enzymes, Transcription Factors, and Phytohormonal Regulators. *Frontiers in Plant Science*, *8*. https://doi.org/10.3389/fpls.2017.00547

Sweetman, C., Deluc, L. G., Cramer, G. R., Ford, C. M., & Soole, K. L. (2009). Regulation of malate metabolism in grape berry and other developing fruits. *Phytochemistry*, *70*(11–12), 1329–1344. https://doi.org/10.1016/j.phytochem.2009.08.006

Terrier, N., & Romieu, C. (2001). Grape Berry Acidity. In K. A. Roubelakis-Angelakis (Ed.), *Molecular Biology & Biotechnology of the Grapevine* (pp. 35–57). Springer Netherlands. https://doi.org/10.1007/978-94-017-2308-4_2

Terrier, Nancy, Glissant, D., Grimplet, J., Barrieu, F., Abbal, P., Couture, C., Ageorges, A., Atanassova, R., Léon, C., Renaudin, J.-P., Dédaldéchamp, F., Romieu, C., Delrot, S., & Hamdi, S. (2005). Isogene specific oligo arrays reveal multifaceted changes in gene expression during grape berry (*Vitis vinifera* L.) development. *Planta*, *222*(5), 832–847. https://doi.org/10.1007/s00425-005-0017-y

Terrier, Nancy, Sauvage, F.-X., Ageorges, A., & Romieu, C. (2001). Changes in acidity and in proton transport at the tonoplast of grape berries during development. *Planta*, *213*(1), 20–28. https://doi.org/10.1007/s004250000472

Terrier, Nancy, Sauvage, F.-X., & Romieu, C. (1996). Absence de crise respiratoire, induction de l' activité alcohol déshydrogénase et diminution de l'acidité vacuolaire lors de la maduration du raisin. *Oenologie 95: 5e. Symposium International d' Oenologie*, 24–28. ISBN 2-7430-0083-X

Tesnière, C., Romieu, C., Dugelay, I., Nicol, M. Z., Flanzy, C., & Robin, J. P. (1994). Partial recovery of grape energy metabolism upon aeration following anaerobic stress. *Journal of Experimental Botany*, *45*(1), 145–151. https://doi.org/10.1093/jxb/45.1.145

Tesnière, Catherine, & Verriès, C. (2000). Molecular cloning and expression of cDNAs encoding alcohol dehydrogenases from *Vitis vinifera* L. during berry development. *Plant Science*, *157*(1), 77–88. https://doi.org/10.1016/S0168-9452(00)00274-0

Thomas, T. R., Shackel, K. A., & Matthews, M. A. (2008). Mesocarp cell turgor in *Vitis vinifera* L. berries throughout development and its relation to firmness, growth, and the onset of ripening. *Planta*, *228*(6), 1067. https://doi.org/10.1007/s00425-008-0808-z

Torregrosa, L. J.-M., Rienth, M., Romieu, C., & Pellegrino, A. (2019). The microvine, a model for studies in grapevine physiology and genetics. *OENO One*, 53(3), Article 3. https://doi.org/10.20870/oeno-one.2019.53.3.2409

Vondras, A. M., Gouthu, S., Schmidt, J. A., Petersen, A.-R., & Deluc, L. G. (2016). The contribution of flowering time and seed content to uneven ripening initiation among fruits within *Vitis vinifera* L. cv. Pinot noir clusters. *Planta*, *243*(5), 1191–1202. https://doi.org/10.1007/s00425-016-2474-x

Zhang, X. Y., Wang, X. L., Wang, X. F., Xia, G. H., Pan, Q. H., Fan, R. C., Wu, F. Q., Yu, X. C., & Zhang, D. P. (2006). A shift of phloem unloading from symplasmic to apoplasmic pathway is involved in developmental onset of ripening in grape berry. *Plant Physiology*, *142*(1), 220–232. https://doi.org/10.1104/pp.106.081430

Zhang, Y., & Keller, M. (2017). Discharge of surplus phloem water may be required for normal grape ripening. *Journal of Experimental Botany*, *68*(3), 585–595. https://doi.org/10.1093/jxb/erw476

Zhu, J., Génard, M., Poni, S., Gambetta, G. A., Vivin, P., Vercambre, G., Trought, M. C. T., Ollat, N., Delrot, S., & Dai, Z. (2019). Modelling grape growth in relation to whole-plant carbon and water fluxes. *Journal of Experimental Botany*, *70*(9), 2505–2521. https://doi.org/10.1093/jxb/ery367

Zouid, I., Siret, R., Jourjon, F., Mehinagic, E., & Rolle, L. (2013). Impact of Grapes Heterogeneity According to Sugar Level on both Physical and Mechanical Berries Properties and Their Anthocyanins Extractability at Harvest. *Journal of Texture Studies*, *44*(2), 95–103. https://doi.org/10.1111/

